Cooperative and Geometry-Dependent Mechanochromic Reactivity through Aromatic Fusion of Two Rhodamines in Polymers

Cooperative and Geometry-Dependent Mechanochromic Reactivity through Aromatic Fusion of Two Rhodamines in Polymers

Mengjiao Wu,[1,2,‡] Yiran Li,[3,‡] Wei Yuan,[2] Guillaume De Bo,*,[4] Yi Cao,*,[3] Yulan Chen*,[1]

[1]State Key Laboratory of Supramolecular Structure and Materials, College of Chemistry, Jilin University, Changchun 130012, P. R. China

[2]Department of Chemistry, Tianjin University, Tianjin 300354, P. R. China

[3]Collaborative Innovation Center of Advanced Microstructures, National Laboratory of Solid State Microstructure, Department of Physics, Nanjing University, Nanjing, 210093, P. R. China

[4]Department of Chemistry, University of Manchester, Oxford Road, Manchester, M13 9PL, UK

ABSTRACT: The unique topological features of Piezo proteins underlie the lever-like cellular mechanotransduction mechanism. This knowledge inspires us to seek topological/geometric control of mechanochromophores with unprecedentedly amplified, synergistic changes in polymers, to serve as ideal stress probes. Here, by judicious placement of two spiro-lactam rings into aminobenzopyranoxanthene, a series of stereo- and regio-isomeric rhodamine-like mechanophores are developed. With two labile bonds closely coupled into one rigidified scaffold, these π-fused bis-mechanophores enable mechanochromic polymers featuring cooperative bond scission, low rupture force (lower than rhodamine), and geometry-controlled ring-opening reactivity. Sonication, single-molecule force spectroscopy experiments, and density functional theory calculations provide insight into the force-color relationship, and rationalize how the difference in reactivity of the four isomeric mechanophores is affected by their molecular geometry and thermodynamic equilibrium. Our strategy based on the aromatic fusion of bis-mechanophore promises a modular approach to isomeric mechanophores for cooperative bond scission. Also, important insights into internal and external factors governing tandem mechanochemical reactions are gained.

INTRODUCTION

Polymer mechanochemistry engages in the coupling of chemical bond scission and macroscopic mechanical response of polymeric materials.[1-4] This vital role is achieved by mechano-responsive polymers, whereby polymer chains are used to conduct force to mechanosensitive groups (mechanophores), activate chemical reactions and break labile chemical bonds.[5-12] Mechanochromic polymers capable of on-demand debonding accompanied with distinct visual signals are particularly attractive since they offer a sensitive platform to quantify mechanochemical reactivity and bond cleavage of overstressed polymer chains.[13-20] Such activation is usually performed on mono-mechanophore-linked polymers or multi-mechanophore-linked polymers,[21-23] either with a low content of labile chemical bonds or low selectivity in bond scission, which limits the magnitude of the overall force response of materials.

In fact, in biological systems, lever-like mechanotransduction mechanism prevails in many physiological processes and underlies diverse vital functions. This mechanism enables the delivery of specific signaling in a transient and amplified way, which mainly relies on the unique topological features of Piezo structures.[24] This knowledge inspires us to seek topological/geometric control of mechanochromophores to achieve amplified, synergistic changes to their molecular and macroscopic proper-

ties. Nowadays, considerable efforts have been devoted to molecular level engineering of the mechanochemical coupling of mechanochromophores.[5,25] For example, the tethered bis-mechanophore design has opened a new avenue toward gradient mechanochromism and tunable mechano-activation (Figure 1a).[26,27] Most bis-mechanophores exhibit different mechanochemical coupling to their mono-mechanophore counterparts: once the first reactive site is activated, the dramatic geometry change tends to reduce the overall mechanochemical reactivity, manifesting two distinct force thresholds (F_{max}). To amplify the desired responses at lower and explicit forces, mechanochromophores in which two reactive sites are activated in a cooperative way (with one F_{max} value) are in high demand. However, except for [4]-ladderane,[28,29] such cooperative mechanophores remain a great challenge. Moreover, recent studies on the regiochemical and stereochemical effects on the activation of spiropyran (SP), naphthopyran (NP) regioisomers, and furan/maleimide adducts have demonstrated disparate activities even when subtle changes were exerted in mechanophore design.[30-32] These findings indicate that both the geometric control of mechanophores and geometric changes involved in bond breaking are critical design elements for mechanophores featuring cooperative bond scission events.

Resembling NP, rhodamine (Rh) can experience a force-induced electrocyclic ring-opening reaction of the twisted spiro-lactam (SL) structure to generate a colored zwitterion
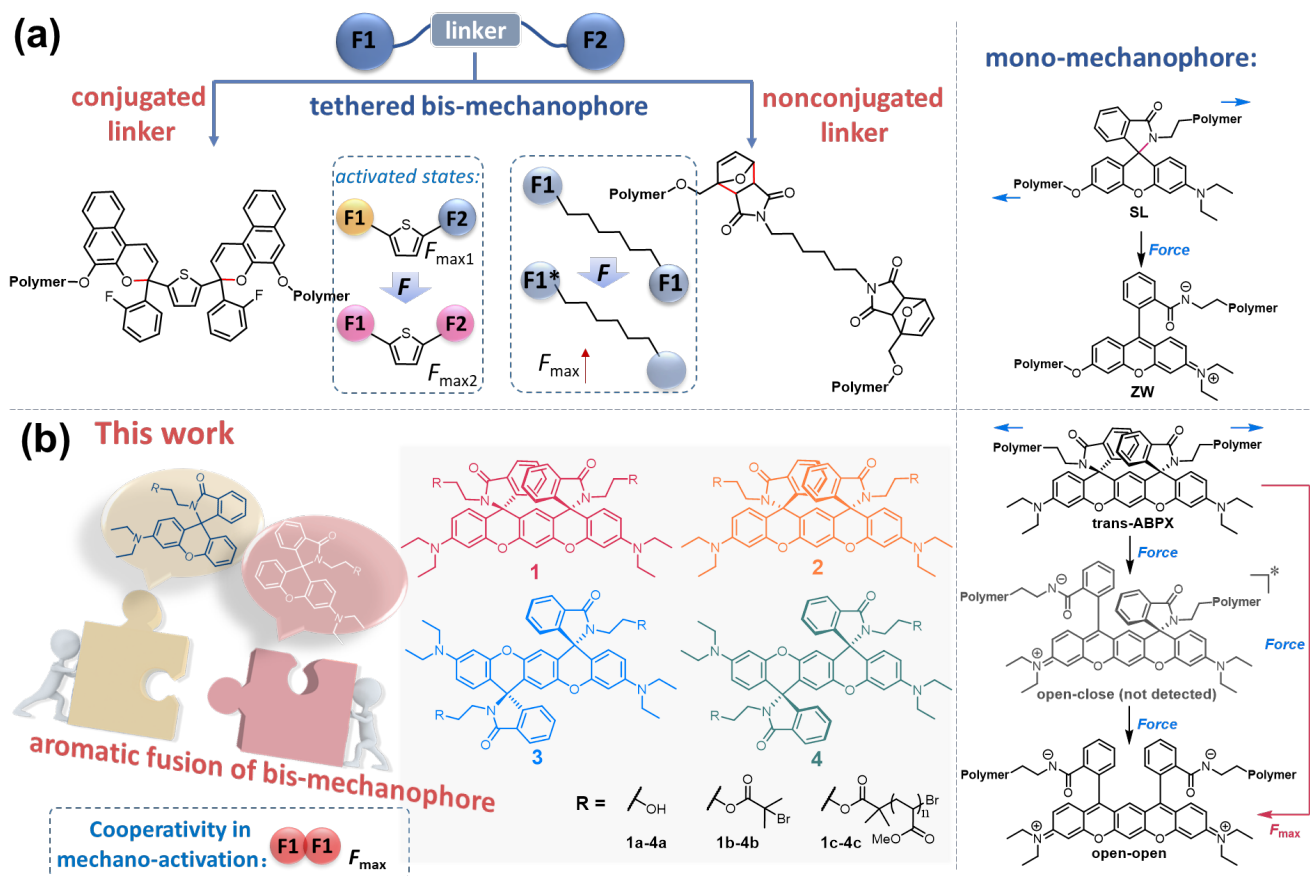
Figure 1. Force-induced ring-opening process from bis-mechanophores. (a) Reported examples of tethered bis-mechanophores: bis-naphthopyran with two F_{max} values (left) and bis-Diels-Alder adduct with higher calculated F_{max} (right); and mono-Rh experiences an electrocyclic ring-opening reaction from SL to ZW state. (b) Strategy and chemical structures designed in this work: four structures are based on π-fused bis-rhodamine mechanophores ABPXs with different configurations (**1**: trans-ABPX; **2**: cis-ABPX; **3**: iso-trans-ABPX; **4**: iso-cis-ABPX). ABPXs experience an electrocyclic ring-opening reaction to ZW state in a cooperative way (taking trans-ABPX for illustration).

(ZW, Figure 1a).[33] Rh is an attractive platform to quantify mechanochemical reactivity because it leads to a simpler ZW product than its NP counterpart (which produces various isomers and conformers).[30,34] So far, mechanochromic studies of Rh-based polymers have mainly focused on bulk materials with little structural variation of the Rh unit,[35] which displayed a low apparent mechanochromic sensitivity. To promote the mechanochromic reactivity of Rh-derived mechanophores, we envisioned that if two spiro-lactam rings were installed in a rigidified skeleton in close proximity, such a fixed configuration would be favorable for its geometry control, promising for cooperativity in the tandem mechanochemical steps (Figure 1b).

Given the sophisticated xanthene chemistry that allows flexible derivatization of the Rh scaffold,[36] we reasoned that judicious placement of spiro-lactam rings into the π-extended xanthene scaffold could facilitate geometry control of Rh-based mechanophores. We herein introduced two mechano-active sites (spiro ring) into one mechanophore in a fused style. Aromatic fusion furnished greater possibilities for mechanophore design, resulting in a family of regio- and stereo-specific mechanochromic isomers (**1-4**, Figure 1b). The mechanochemical reactivities of the corresponding poly(methacrylates) (PMA) were exploited as functions of molecular geometry, environmental polarity, and the manifestation of mechanochemistry.

Impressively, as for all the isomeric polymers, both experimental and theoretical results from sonication, single-molecule force spectroscopy, and density functional theory (DFT) calculation verified the cooperative ring-opening reactions triggered by the lowered force threshold, in contrast to NP and Rh polymers. Also, the remarkably different mechanochromic reactivities from this kind of isomeric aminobenzopyranoxanthene (ABPX)-based mechanophores were illuminated in terms of geometry and thermodynamic equilibrium. The success of these π-fused mechanochromophores will not only inspire the modular preparation of stress-sensing polymers with amplified responses, but also offer abundant opportunities to advance the fundamental understanding of mechanochemical reactivity, which is underdeveloped in comparison to other areas of organic chemistry.

RESULTS

We targeted a set of ABPX-centered chromophores that contain two spirolactam rings fused into either C_{2v} or C_{2h} structures. The four mechanochromophores can be regarded as π-fused bis-rhodamine analogs. Such mechanophore design was inspired by the facile synthesis of fused ABPX dyes based on the condensation of benzophenone derivative with hydroquinone or resorcinol in concentrated H_2SO_4 at 100 °C to generate regio isomers with different symmetries (trans/cis-ABPX and iso-trans/cis-

ABPX, Figure S1).[37-39] Both ABPX and iso-ABPX intermediates have isomers arising from the configuration of two spiro rings. In the trans forms (**1** and **3**), the two lactone carbonyl groups are on the opposite faces of the xanthene ring, whereas these groups are on the same face in the cis forms (**2** and **4**). The two forms could be separated by silica-gel chromatography.[39] Then, the respective four regio- and stereo- isomers were converted into the corresponding bis-hydroxyl and bis-α-bromo-ester functionalized lactam-isomers as monomers (**1a-4a**) for polycondensation or initiators (**1b-4b**) for single-electron transfer-living radical polymerization, affording ABPX-containing segmented polyester (**P1-P4**, Figure S3) or ABPX-linked PMA (**1c-4c**, Figure S4) respectively. Due to the steric hindrance of the spiro rings and the rigidity of the ABPX scaffold, the geometries of these isomers were conserved in the subsequent reactions, which were unambiguously characterized by ^{1}H NMR, ^{13}C NMR, and MALDI-TOF spectroscopy (details in SI). End-functionalized PMA and Rh-linked PMA were also synthesized as control polymers (Figures S2, S5, and Table S1).
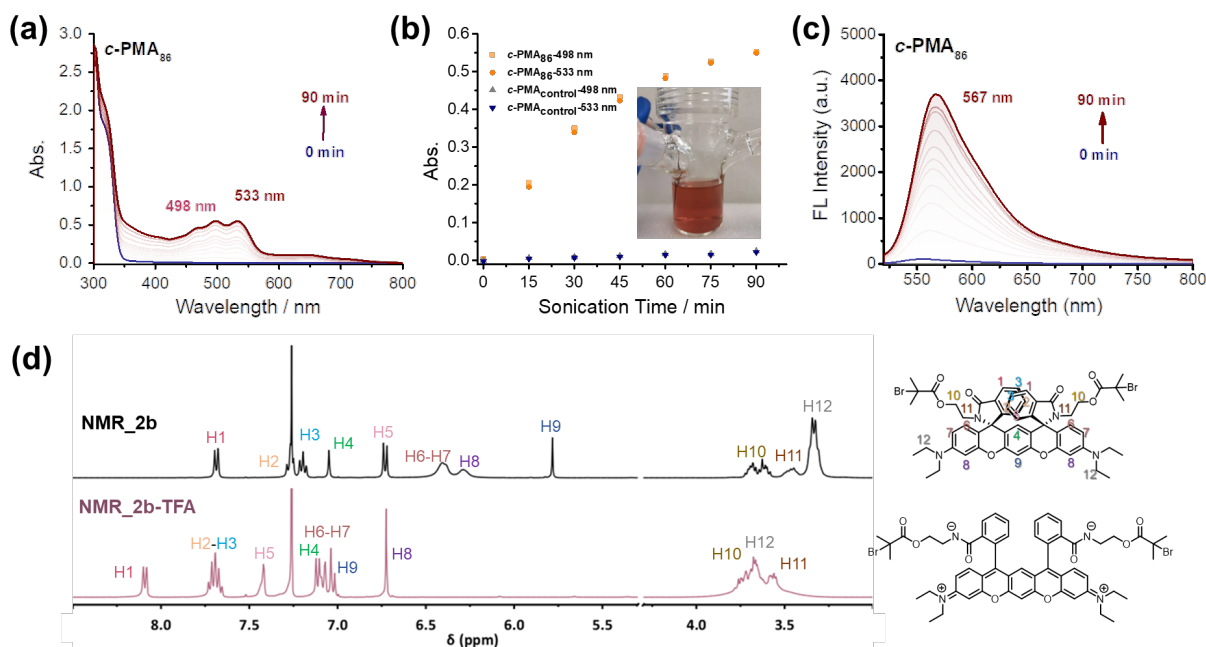

Figure 2. Mechanochromism from ABPX-linked PMAs by ring-opening reaction of ABPX mechanophore. (a) Representative UV-vis spectra of *c*-PMA$_{86}$ (**2c**, M_n = 86.3 kDa) under pulsed sonication in MeCN; (b) the corresponding absorbance monitored at 498 nm and 533 nm for *c*-PMA$_{86}$ and end-functionalized polymer *c*-PMA$_{control}$ (M_n = 70.7 kDa); insert shows the chromic solution *c*-PMA$_{86}$ after sonication; (c) the corresponding FL emission spectra (λ_{ex} = 500 nm); (d) ^{1}H NMR spectra of the corresponding small molecule **2b** before (above) and after (below) addition of excess trifluoroacetic acid (TFA).

We performed the mechanical activation of these ABPX-linked PMAs in N,N-dimethylformamide (DMF) or acetonitrile (MeCN) at 0 °C, using pulsed sonication (1s ON, 1s OFF; 25-29 W). All solutions changed gradually from colorless to red with the emergence of new UV-vis absorption peaks in the long wavelength region (533 and 555 nm for **1c/2c** in DMF, 498 nm and 533 nm for **1c/2c** in MeCN; 525 nm and 550 nm for **3c/4c** in DMF; 519 nm and 544 nm for **3c/4c** in MeCN, Figures 2a, 2b, S6-S10). Additionally, the absorption peak beyond 600 nm was mostly derived from the aggregation of negative and positive charged zwitterions,[37,38] which is also supported by the proposed mechanism of selective and heterolytic scission of C-N bonds (Figure 1b). A similar chromic effect was observed for the acidified solutions of small molecules **2b** and **4b** (Figure S24), featuring the characteristic peaks at 533 and 544 nm as well, whereas no peak beyond 600 nm was observed due to the shielding effect of the negative charge (CF$_3$COO$^-$).[40] Meanwhile, NMR spectra of the acid-chromic solutions of **2b** and **4b** manifested their peaks either shifting downfield (aromatic protons) or being less resolved (-NCH$_2$-), corresponding to the explicit formation of an open-open form with a π-extended skeleton (Figures 2d, S25, S26).[41] In contrast, the optical properties of the control PMA solutions did not change under sonication (Figures 2b, S11). These observations confirmed that the color change in polymer **1c-4c** under sonication was due to the mechanically induced ring-opening of spirolactams, affording the open-open species.

Previous reports on the chemical stimuli of spironolactone containing ABPXs have demonstrated a stepwise structural and chromic conversion.[42] In contrast, according to UV-vis absorption spectra, the quick formation of open-open species under sonication indicated that the mechanical activation of the four ABPX-linked polymers might occur via different mechanisms. This inference could also be verified experimentally by monitoring the fluorescent property of the ultrasonic solutions. Only when the two spiro rings were opened simultaneously, ABPX-based molecules could emit fluorescence due to the restricted process of photo-induced electron transfer (Figure S13).[42] The fluorescence spectra recorded during sonication displayed turn-on emission at the initial stage (567 nm for 1c/2c; 564 nm for 3c/4c; Figures 2c, S14-S18). Therefore, the two spiro rings were opened in a cooperative manner or the open-open species emerged much more quickly than the open-close intermediates.
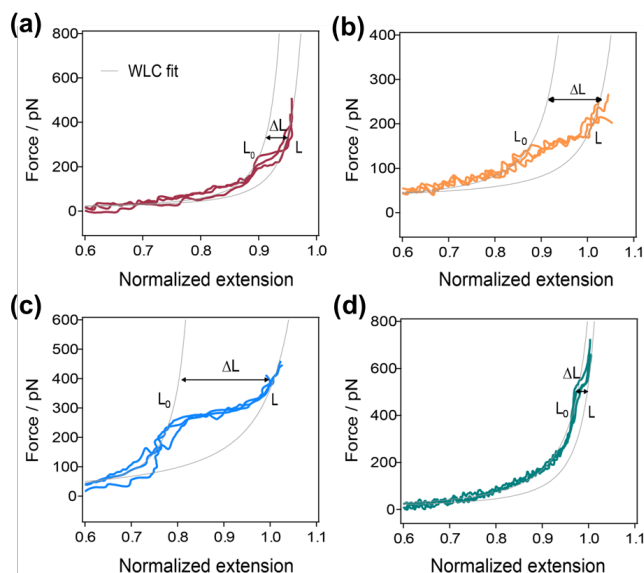
Figure 3. SMFS results for ABPX containing segmented polymers. Representative force-extension curves with worm-like chain (WLC) of (a) **P1** ($\Delta L = 28.3 \pm 20.2$ Å); (b) **P2** ($\Delta L = 31.7 \pm 12.3$ Å); (c) **P3** ($\Delta L = 40.7 \pm 35.3$ Å); (d) **P4** ($\Delta L = 24.0 \pm 12.9$ Å).

Next, the single-molecule force spectroscopy (SMFS) technique based on atomic force microscopy was employed to study the mechanochemical reactivity of ABPX containing segmented polyesters **P1-P4** at a single molecular level (details in SI). The pickup rate was kept as low as ~0.5% to ensure a single molecule was stretched each time. As shown in Figure 3, when **P1-P4** were pulled in DMF at a pulling speed of 400 nm/s, the well-overlapped curves after normalization indicated that these force-extension curves were from the similar single polymer chains (the complete curves in Figure S27). The force plateaus suggested that the polymer chains were elongated at given forces due to the force-induced activation of the mechanophores. The distinct contour length changes (ΔL) of the polymers matched with the expected length changes of the mechanophores. In the force-extension curves of all polymers, only a single plateau was observed, indicating the cooperative ring-opening dominated the fracture mechanism of the mechanophores in **P1-P4** (Figure S28 and Table S2). If the two spirolactam rings were opened sequentially, we would otherwise observe two force plateaus. Note that, the activation forces for these mechanophores were in a range of 200-600 pN, significantly lower than the rupture force of most mechanophores reported in literature, such as cyclopropanes, benzocyclobutenes, and organometallic mechanophores but similar to spiropyrans.[7,43-45] The SMFS experiments confirmed the successful conversion of ring-opening isomerization of the four ABPX-based mechanophores.
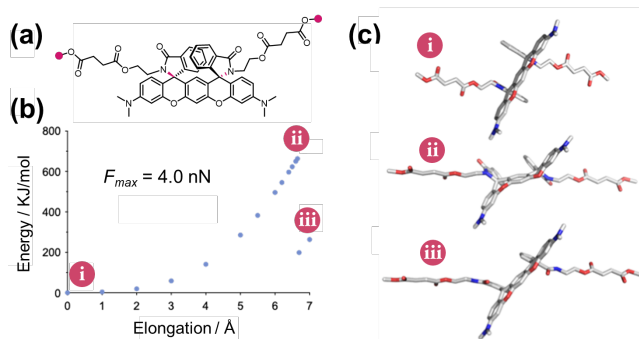

Figure 4. Simulated elongation of trans-ABPX mechanophore. The elongation of a model of trans-APBX **1** (a) was simulated (b) using the CoGEF method (DFT, B3LYP/6-31G*, C-PCM dielectric = 37.22 (DMF)). Anchors atoms are highlighted with pink disk. Scissile bonds are shown in red. (c) Equilibrium geometries at onset (i), maximal deformation (ii), and after scission (iii).

The reaction details of **1-4** were simulated by Constrained Geometry Simulates External Force (CoGEF) calculations (DFT B3LYP/6-31G*) with an implicit polar solvent model (dielectric = 37.22, equal to DMF, Figures 4, S29). For all four isomers, their two spirolactam rings exhibited C-N bond cleavage synergistically with only one rupture force value (F_{max}) detected for each isomer (Figure S29). This finding was different from that of bis-NP, which showed two discrete rupture force values.[26] Notably, the geometric change from the highly twisted closed state to zwitterions products with the resultant xanthene scaffold unexpectedly bent to different extents was validated. The simulated F_{max} and force-free end-to-end contour length change (Δx) can be determined from the CoGEF calculations (Table S3, Figures S30-S33) and discussed according to the Van't Hoff equation:[46]

$$\frac{d \ln K}{dF} = \frac{\Delta x}{kT} \qquad \text{(Eq. 1)}$$

Where T is reaction temperature, K is the equilibrium constant, k is the rate constant, Δx is the distance between the pulling points in the product and reactant state. F_{max} for **1-4** was predicted in the region of 3.4-4.2 nN, lower than those of Rh (4.3 nN) and NP (4.1-4.3 nN).[47] This lowered force value indicated a promoted mechanochemical coupling, which was different from other documented tethered bis-mechanophores,[26,27] and again, proved the cooperative bond rupture manner. In this way, the enhanced force sensitivity of these newly explored aromatic fused mechanophores was highlighted.

It is worth mentioning that, in contrast to SP and NP, under the conventional computational model, a rearrangement occurred spontaneously after the scission of the C-N bond in one of the lactam rings.[47] In the presence of a polarizable continuum model, heterolytic cleavage of the two C-N bonds could be observed without any rearrangement (Figure 4). These results implied that the ring-opening structures of **1-4** were highly polarized and that the opening-closing equilibrium was sensitive to the polarity of solvents, in line with experimental findings.
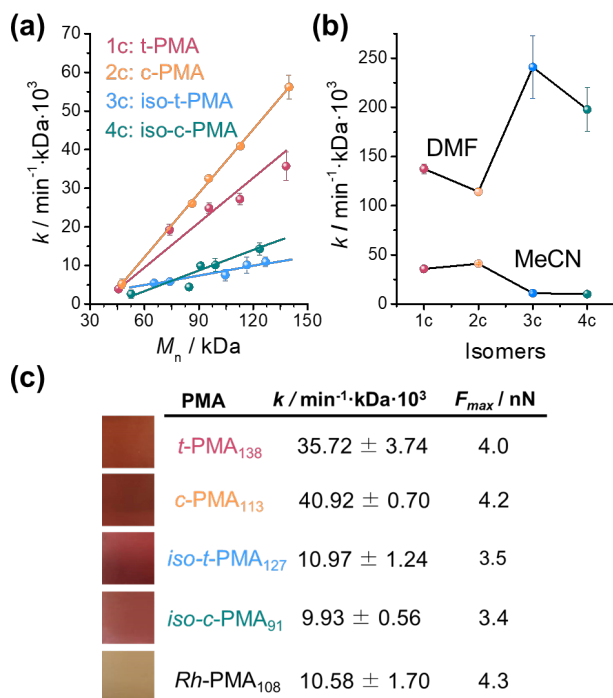
Figure 5. Comparison of mechanochromic reactivity of the four kinds of isomeric polymers. (a) Rate constant k of mechanochemical activation of **1c-4c** as a function of the molecular weight M_n in MeCN; (b) k for **1c-4c** (**t-PMA$_{138}$**; **c-PMA$_{113}$**; **iso-t-PMA$_{127}$**; **iso-c-PMA$_{91}$**) activated in DMF and MeCN (Error bars represent the standard deviation; details in the SI). (c) Summary of the chromic solutions after sonication in MeCN and the k (determined by sonication experiment) and F_{max} (determined by CoGEF calculation) values for different mechanophores.

Apart from the cooperative feature in these tandem mechanochromic reactions, the geometry-dependent mechanochromic reactivity was also detected. The fact that two spiro-rings were broken cooperatively facilitated quantitative analysis of the overall mechanochemical reactivity of different polymers. The ring-opening reaction rates of different sonicated polymer solutions were established according to the variation in UV absorbance of the corresponding characteristic peak. Taking those in MeCN as an example, the absorbance plots of 533 nm for **1c/2c** and 544 nm for **3c/4c** versus sonication time were well fitted to the first-order dynamic equation:[48]

$$A = B*(1-\exp(-k*t)) \quad \text{(Eq. 2)}$$

where A is the absorbance at time t, and B is the amplitude (the maximum absorbance value). After non-linear fitting, the rate constant k of each PMA can be accessed (Figures S19-S23). As summarized in Figure 5a, for each isomer, linear fitting of k values against the corresponding molecular weight revealed the positive effect of M_n on the rate of mechanochemical reaction, which was a typical feature in mechano-responsive polymers and further identified the mechanical origin of the observed ultrasound-induced reactivity.[49] Impressively, for the same batch of polymers, sonication in DMF led to a much faster reaction

rate than that in MeCN (Figure 5b). Moreover, in the same solvent, **1c-4c** were different from each other in their activation rates, whose trends were also solvent-dependent. In DMF, the reactivity of **3c/4c** was distinctly higher than that of **1c/2c**. Whereas in MeCN, it seemed that mechanically induced ring-opening of **1c/2c** was somehow accelerated and surpassed **3c/4c** (Figure 5b). The isomeric effect on mechanophore activation was also uncovered by SMFS tests and CoGEF simulation, illustrating different contour length increments (ΔL), displacements (Δx), and rupture force values (F_{max}) from **1-4** (Figures S30-S33 and Table S2).

Lastly, when compared to the mono-mechanophore counterpart **Rh-PMA$_{108}$**, sonication-induced cooperative chromism from the four ABPX-linked polymers with resembling M_n was more appreciable. Moreover, the reaction rate of ABPX-linked PMA (**1c** and **2c**) increased remarkably (Figure S12). The red color of **1c-4c** was persistent after a plateau was reached under sonication. Slow reversion into colorless ones was observed after the sonicated solutions were left under ambient condition for several days, corresponding to the reversible transition of spiro rings between the SL and ZW states. Altogether, these evidences highlighted the strength of the multi-aromatic fusion strategy in mechanophore design to create mechanochromic materials with high sensitivity.

DISCUSSION

The results presented here provide valuable insights into the molecular mechanochromic response associated with the rhodamine analog mechanophores. First, all the experimental and theoretical studies have identified the unique cooperativity in bond scission steps and the increase in mechano-sensitivity of the four mechanophores, compared to the mono-Rh counterpart (Figure 5c). Such positive mechanochemical coupling behaviors very likely benefit from the structural characteristics of these new mechanophores possessing rigid π-extended scaffolds and two scissile bonds in close proximity. These findings reflect the strength of our design strategy based on the aromatic fusion of the bis-mechanophore. Second, the mechanochromic reactivity of these ABPX mechanophores is stereo- and regiospecific, as well as solvent dependent. Similar to Rh and SP, in principle, the ring-opening reactions of the four mechanophores can be affected by thermodynamic equilibrium, by which force coupled reaction equilibrium substantially determines the mechanochromic reactivity. In DMF, sonication experiments and DFT calculations led to a similar trend of the geometry-dependent mechanical susceptibility, which was in accordance with different geometrical changes under force (referring to Eq. 1).

Moreover, the origin of the solvent-sensitive response might be found by looking at the additional electronic effect. Once the first spiro-ring is broken, the intermediate zwitterion is not stable, which can accelerate the reaction and shift the equilibrium to a more polarized bis-zwitterion. This can contribute to explaining why the open-open species appear
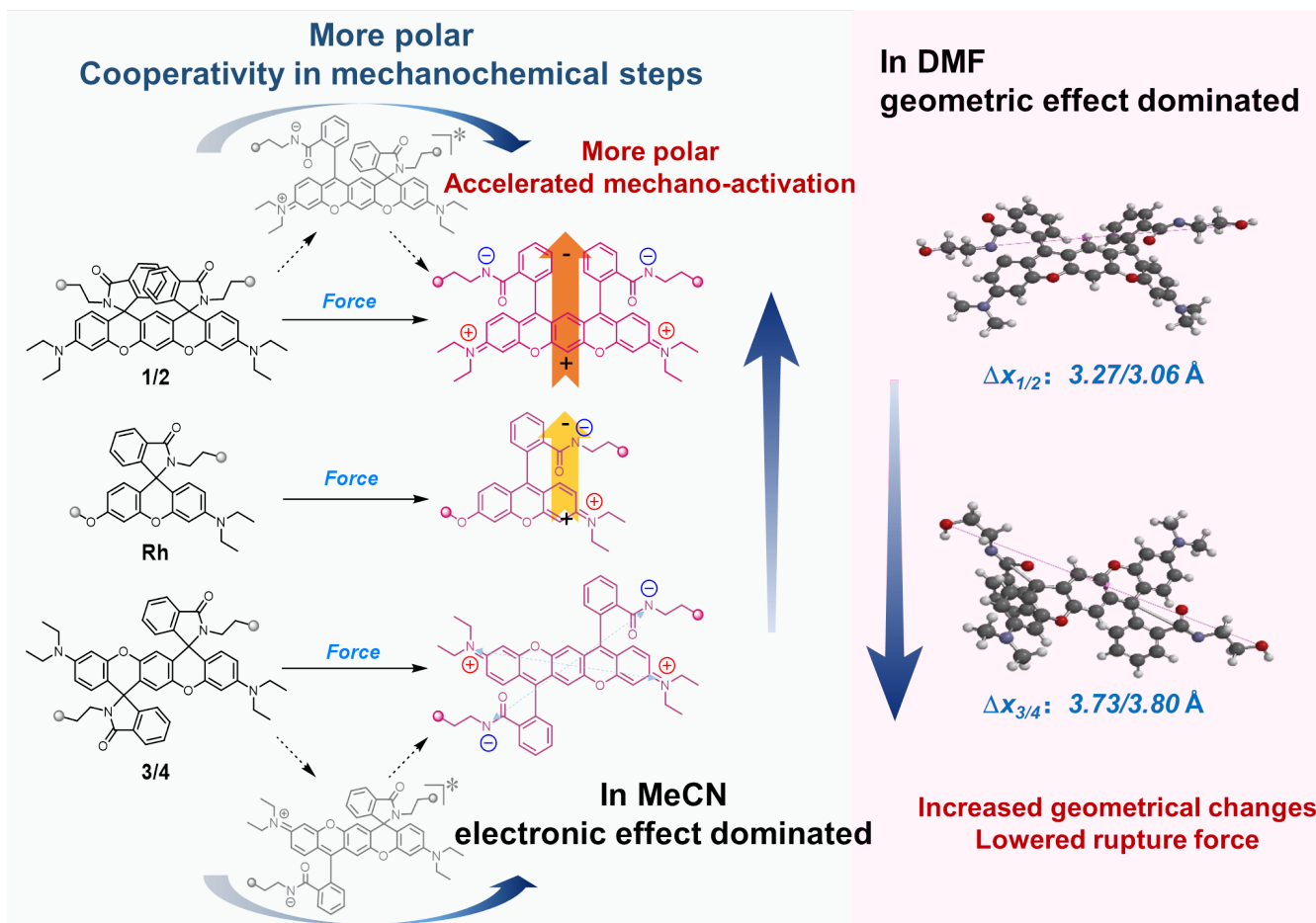
Figure 6. Proposed mechanism for different mechanochromic reactivity among the regio-isomers, stereo-isomers and mono-Rh counterpart. Dominated by electronic effect in MeCN *vs* dominated by geometric effect in DMF.

to be generated directly from ABPX without the detection of open-close intermediates. It may also be rationalized that the mechanochemical reactions are faster in a more polarized substrate, eg, **1/2** *vs* pristine Rh, and in more polar DMF *vs* in MeCN.[50,51] Besides, the relatively low vapor pressure of DMF may be partial contribution of the increased rate constant.[49] Notably in MeCN, the acceleration of **1/2** over **3/4** was detected. Unlike **3** and **4**, which produce centrosymmetric zwitterions where the dipole cancels each other, the activation of **1** and **2** leads to a zwitterion with parallel dipoles, which might impose a significant electronic/polarizing effect on the SL-ZW equilibrium. Therefore, if only electronic effects were at play, the more polar ZW of **1/2** would be favorably formed in a polar environment (eg, in DMF, as well as in MeCN and bulk sample as a relatively low polar environment to DMF, Figure S34).[17] However in DMF, the isomer-dependent polarizing impact on their mechanochromic activity seemed negligible, which was otherwise dominated by the distinct geometrical changes. In other words, we speculate that the mechanochemical coupling and electronic effect play different and complex roles on the mechanochemical reactivity, depending on the mechanophores and solvents used. The joint effects herein might differentially alter the activation rate between **1/2** and **3/4**. Whereas the different trends detected from SMFS might be ascribed to different loading velocities and polymer backbones. A notable bias of rupture force between the SMFS and CoGEF results has also been discovered for SP mechanophores,[45,47] perhaps due to the time scale gap between experiment and calculation.[52]

Accordingly, the molecular origins of the different activation behaviors of these π-extended bis-mechanophores are speculated in Figure 6, which depicted the mechanochromism of ABPX-containing polymers as a mechanically triggered electronically auto-acceleration process, causing cooperativity in the tandem mechanochemical steps. Indeed, this picture could also elucidate our finding that the discrepancy of activity caused by regio-isomers exceeds that of stereoisomers.

CONCLUSION

To conclude, a set of fused ABPXs containing polymers that exhibit cooperative, geometry-dependent mechanochromism has been developed. The key to the success of this mechanochemistry is the aromatic fusion of two reactive sites (rhodamine ring) into one mechanophore, allowing for stereo- and regio-selective synthesis of isomeric mechanophores with pronounced mechanochromic sensitivity. These stereo- and regio-isomeric polymers displayed greatly varied mechanochromic reactivity, which was mainly due to the different force-coupled geometry changes alongside the polarity enhancement. These findings suggested the importance of both geometric and polar (thermodynamic equilibrium) control of mechano-responsive polymers. Importantly, the current design based on the aromatic fusion of bis-mechanophore and the mechanistic insights into the respective consecutive mechano-activations will aid the future development of mechanochromic materials with the potentially amplified responses and controlled products.

ASSOCIATED CONTENT

Supporting Information

General experimental details; synthetic details; sonication experiments; acid response of initiators; single molecule force spectroscopy experiments; CoGEF calculations; tensile tests; NMR spectra. This material is available free of charge via the Internet at http://pubs.acs.org."

AUTHOR INFORMATION

Corresponding Authors

Yulan Chen - State Key Laboratory of Supramolecular Structure and Materials, College of Chemistry, Jilin University, Changchun, 130012, China;
https://orcid.org/0000-0001-6017-8888;
Email: yulanchen@jlu.edu.cn

Guillaume De Bo - School of Chemistry, University of Manchester, Oxford Road, Manchester M13 9PL, United Kingdom;
http://orcid.org/0000-0003-2670-6370;
Email: guillaume.debo@manchester.ac.uk

Yi Cao - Collaborative Innovation Center of Advanced Microstructures, National Laboratory of Solid State Microstructure, Department of Physics, Nanjing University, Nanjing 210093, China;
https://orcid.org/0000-0003-1493-7868;
Email: caoyi@nju.edu.cn

Authors

Mengjiao Wu - State Key Laboratory of Supramolecular Structure and Materials, College of Chemistry, Jilin University, Changchun, 130012, People's Republic of China; Tianjin Key Laboratory of Molecular Optoelectronic Sciences, Department of Chemistry, School of Science, Tianjin University, Tianjin 300072, China

Yiran Li - Collaborative Innovation Center of Advanced Microstructures, National Laboratory of Solid State Microstructure, Department of Physics, Nanjing University, Nanjing 210093, China;

Wei Yuan - Tianjin Key Laboratory of Molecular Optoelectronic Sciences, Department of Chemistry, School of Science, Tianjin University, Tianjin 300072, China

Author Contributions

‡M.W. and Y.L. contributed equally to this work.

Notes

The authors declare no competing financial interest.

ACKNOWLEDGMENT

REFERENCES

(1) Stratigaki, M.; Göstl, R. Methods for Exerting and Sensing Force in Polymer Materials Using Mechanophores. *ChemPlusChem* **2020**, *85*, 1095-1103.

(2) Ghanem, M. A.; Basu, A.; Behrou, R.; Boechler, N.; Boydston, A. J.; Craig, S. L.; Lin, Y.; Lynde, B. E.; Nelson, A.; Shen, H.; Storti, D. W. The Role of Polymer Mechanochemistry in Responsive Materials and Additive Manufacturing. *Nat. Rev. Mater.* **2021**, *6*, 84-98.

(3) Ducrot, E.; Chen, Y.; Bulters, M.; Sijbesma, R. P.; Creton, C. Toughening Elastomers with Sacrificial Bonds and Watching Them Break. *Science* **2014**, *344*, 186-189.

(4) Willis-Fox, N.; Rognin, E.; Aljohani, T. A.; Daly, R. Polymer Mechanochemistry: Manufacturing Is Now a Force to Be Reckoned With. *Chem* **2018**, *4*, 2499-2537.

(5) Chen, Y.; Mellot, G.; Luijk, D.; Creton C.; Sijbesma, R. P. Mechanochemical Tools for Polymer Materials. *Chem. Soc. Rev.* **2021**, *50*, 4100-4140.

(6) Nixon, R.; De Bo, G. Three Concomitant C-C Dissociation Pathways during the Mechanical Activation of an N-heterocyclic Carbene Precursor. *Nat. Chem.* **2020**, *12*, 826-831.

(7) Yang, Y.; Wang, A.; Kouznetsova, T. B.; Sha, Y.; Xu, E.; Shannahan, L.; Fermen-Coker, M.; Lin, Y.; Tang, C.; Craig, S. L. Distal Conformational Locks on Ferrocene Mechanophores Guide Reaction Pathways for Increased Mechanochemical Reactivity. *Nat. Chem.* **2021**, *13*, 56-62.

(8) Huo, S.; Zhao, P.; Shi, Z.; Zou, M.; Yang, X.; Warszawik, E.; Loznik, M.; Göstl, R.; Herrmann, A. Mechanochemical Bond Scission for the Activation of Drugs. *Nat. Chem.* **2021**, *13*, 131-139.

(9) Li, J.; Nagamani, C.; Moore, J. S. Polymer Mechanochemistry: From Destructive to Productive. *Acc. Chem. Res.* **2015**, *48*, 2181-2190.

(10) Hu, X.; McFadden, M. E.; Barber, R. W.; Robb, M. J. Mechanochemical Regulation of a Photochemical Reaction. *J. Am. Chem. Soc.* **2018**, *140*, 14073-14077.

(11) Akbulatov, S.; Boulatov, R. Experimental Polymer Mechanochemistry and its Interpretational Frameworks. *ChemPhysChem* **2017**, *18*, 1422-1450.

(12) Larsen, M. B.; Boydston, A. J. "Flex-Activated" Mechanophores: Using Polymer Mechanochemistry to Direct Bond Bending Activation. *J. Am. Chem. Soc.* **2013**, *135*, 8189-8192.

(13) Chen, Y.; Spiering, A. J. H.; Karthikeyan, S.; Peters, G. W. M.; Meijer, E. W.; Sijbesma, R. P. Mechanically Induced Chemiluminescence from Polymers Incorporating a 1,2-Dioxetane Unit in the Main Chain. *Nat. Chem.* **2021**, *4*, 559-562.

(14) Shi, Z.; Song, Q.; Göstl, R.; Herrmann, A. The Mechanochemical Release of Naphthalimide Fluorophores from β-Carbonate and β-Carbamate Disulfide-Centered Polymers. *CCS Chem.* **2021**, *3*, 2333-2344.

(15) Yang, F.; Li, X.; Chen, Y. A Chromic and Near-Infrared Emissive Mechanophore Serving as a Versatile Force Meter in Micelle-Hydrogel Composites. *Adv. Opt. Mater.* **2022**, *10*, 2102552.

(16) Wu, M.; Guo, Z.; He, W.; Yuan, W.; Chen, Y. Empowering Self-Reporting Polymer Blends with Orthogonal Optical Properties Responsive in a Broader Force Range. *Chem. Sci.* **2021**, *12*, 1245-1250.

(17) Qi, Q.; Sekhon, G.; Chandradat R.; Ofodum, N. M.; Shen, T.; Scrimgeour, J.; Joy, M.; Wriedt, M.; Jayathirtha, M.; Darie, C. C.; Shipp, D. A.; Liu, X.; Lu, X. Force-Induced Near-Infrared Chromism of Mechanophore-Linked Polymers. *J. Am. Chem. Soc.* **2021**, *143*, 17337-17343.

(18) Kosuge, T.; Zhu, X.; Lau, V. M.; Aoki, D.; Martinez, T. J.; Moore, J. S.; Otsuka, H. Multicolor Mechanochromism of a Polymer/Silica Composite with Dual Distinct Mechanophores. *J. Am. Chem. Soc.* **2019**, *141*, 1898-1902.

(19) Sagara, Y.; Karman, M.; Verde-Sesto, E.; Matsuo, K.; Kim, Y.; Tamaoki, N.; Weder, C. Rotaxanes as Mechanochromic Fluorescent Force Transducers in Polymers. *J. Am. Chem. Soc.* **2018**, *140*, 1584-1587.

(20) Watabe, T.; Aoki, D.; Otsuka, H. Enhancement of Mechanophore Activation in Mechanochromic Dendrimers by Functionalization of Their Surface. *Macromolecules* **2012**, *54*, 1725-1731.

(21) Potisek, S. L.; Davis, D. A.; Sottos, N. R.; White, S. R.; Moore, J. S. Mechanophore-linked Addition Polymers. *J. Am. Chem. Soc.* **2007**, *129*, 13808-13809.

(22) Davis, D. A.; Hamilton, A.; Yang, J.; Cremar, L. D.; Gough, D. V.; Potisek, S. L.; Ong, M. T.; Braun, P. V.; Martínez, T. J.; White, S. R.; Moore, J. S.; Sottos, N. R. Force-Induced Activation of Covalent Bonds in Mechanoresponsive Polymeric Materials. *Nature* **2009**, *459*, 68-72.

(23) Bowser, B. H.; Craig, S. L. Empowering Mechanochemistry with Multimechanophore Polymer Architectures. *Polym. Chem.* **2018**, *9*, 3583-3593.

(24) Zhao, Q.; Zhou, H.; Chi, S.; Wang, Y.; Wang, J.; Geng, J.; Wu, K.; Liu, W.; Zhang, T.; Dong, M.; Wang, J.; Li, X.; Xiao, B. Structure and Mechanogating Mechanism of the Piezo1 Channel. *Nature* **2018**, *554*, 487-492.

(25) He, S.; Stratigaki, M.; Centeno, S. P.; Dreuw, A.; Göstl, R. Tailoring the Properties of Optical Force Probes for Polymer Mechanochemistry. *Chem. Eur. J.* **2021**, *27*, 15889-15897.

(26) McFadden, M. E.; Robb, M. J. Force-Dependent Multicolor Mechanochromism from a Single Mechanophore. *J. Am. Chem. Soc.* **2019**, *141*, 11388-11392.

(27) Stevenson, R.; Zhang, M.; De Bo, G. Mechanical Activation of Polymers Containing Two Adjacent Mechanophores. *Polym. Chem.* **2020**, *11*, 2864-2868.

(28) Chen, Z.; Zhu, X.; Yang, J.; Mercer, J. A. M.; Burns, N. Z.; Martinez, T. J.; Xia, Y. The Cascade Unzipping of Ladderane Reveals Dynamic Effects in Mechanochemistry. *Nat. Chem.* **2020**, *12*, 302-309.

(29) Chen, Z.; Mercer, J. A. M.; Zhu, X.; Romaniuk, J. A. H.; Pfattner, R.; Cegelski, L.; Martinez, T. J.; Burns, N. Z.; Xia, Y. Mechanochemical Unzipping of Insulating Polyladderene to Semiconducting Polyacetylene. *Science* **2017**, *357*, 475-479.

(30) Lin, Y.; Barbee, M. H.; Chang, C.; Craig, S. L. Regiochemical Effects on Mechanophore Activation in Bulk Materials. *J. Am. Chem. Soc.* **2018**, *140*, 15969-15975.

(31) Robb, M. J.; Kim, T. A.; Halmes, A. J.; White, S. R.; Sottos, N. R.; Moore, J. S. Regioisomer-Specific Mechanochromism of Naphthopyran in Polymeric Materials. *J. Am. Chem. Soc.* **2016**, *138*, 12328-12331.

(32) Stevenson, R.; De Bo, G. Controlling Reactivity by Geometry in Retro-Diels-Alder Reactions under Tension. *J. Am. Chem. Soc.* **2017**, *139*, 16768-16771.

(33) Wang, Z.; Ma, Z.; Wang, Y.; Xu, Z.; Luo, Y.; Wei, Y.; Jia, X. A Novel Mechanochromic and Photochromic Polymer Film: When Rhodamine Joins Polyurethane. *Adv. Mater.* **2015**, *27*, 6469-6474.

(34) Inagaki, Y.; Kobayashi, Y.; Mutoh, K.; Abe, J. A Simple and Versatile Strategy for Rapid Color Fading and Intense Coloration of Photochromic Naphthopyran Families. *J. Am. Chem. Soc.* **2017**, *139*, 13429-13441.

(35) Wang, T.; Zhang, N.; Dai, J.; Li, Z.; Bai, W.; Bai, R. Novel Reversible Mechanochromic Elastomer with High Sensitivity: Bond Scission and Bending-Induced Multicolor Switching. *ACS Appl. Mater. Interfaces* **2017**, *9*, 11874-11881.

(36) Luo, X.; Qian, L.; Xiao, Y.; Tang, Y.; Zhao, Y.; Wang, X.; Gu, L.; Lei, Z.; Bao, J.; Wu, J.; He, T.; Hu, F.; Zheng, J.; Li, H.; Zhu, W.; Shao, L.; Dong, X.; Chen, D.; Qian, X.; Yang, Y. A Diversity-Oriented Rhodamine Library for Widespectrum Bactericidal Agents with Low Inducible Resistance Against Resistant Pathogens. *Nat. Commun.* **2019**, *10*, 258.

(37) Kamino, S.; Muranaka, A.; Murakami, M.; Tatsumi, A.; Nagaoka, N.; Shirasaki, Y.; Watanabe, K.; Yoshida, K.; Horigome, J.; Komeda, S.; Uchiyama, M.; Enomoto, S. A Red-Emissive Aminobenzopyrano-Xanthene Dye: Elucidation of Fluorescence Emission Mechanisms in Solution and in the Aggregate State. *Phys. Chem. Chem. Phys.* **2013**, *15*, 2131-2140.

(38) Kamino, S.; Horio, Y.; Komeda, S.; Minoura, K.; Ichikawa, H.; Horigome, J.; Tatsumi, A.; Kaji, S.; Yamaguchi, T.; Usami, Y.; Hirota, S.; Enomoto, S.; Fujita, Y. A New Class of Rhodamine Luminophores: Design, Syntheses and Aggregation-Induced Emission Enhancement. *Chem. Commun.* **2010**, *46*, 9013-9015.

(39) Shirasaki, Y., Kamino, S., Tanioka, M., Watanabe, K., Takeuchi, Y., Komeda, S., Enomoto, S. New Aminobenzopyranoxanthene-Based Colorimetric Sensor for Copper(II) Ions with Dual-Color Signal Detection System. *Chem. Asian J.* **2013**, *8*, 2609-2613.

(40) Belov, V. N.; Bossi, M. L.; Fölling, J.; Boyarskiy, V. P.; Hell, S. W. Rhodamine Spiroamides for Multicolor Single-Molecule Switching Fluorescent Nanoscopy. *Chem. Eur. J.* **2009**, *15*, 10762-1077.

(41) Qian, H.; Purwanto, N. S.; Ivanoff, D. G.; Halmes, A. J.; Sottos, N. R.; Moore, J. S. Fast, Reversible Mechanochromism of Regioisomeric Oxazine Mechanophores: Developing in situ Responsive Force Probes for Polymeric Materials. *Chem* **2021**, *7*, 1080-1091.

(42) Wang, C; Wong, K. M. Selective Hg^{2+} Sensing Behaviors of Rhodamine Derivatives with Extended Conjugation Based on Two Successive Ring-Opening Processes. *Inorg. Chem.* **2013**, *52*, 13432-13441.

(43) Klukovich, H. M.; Kouznetsova, T. B.; Kean, Z. S.; Lenhardt, J. M.; Craig, S. L. A Backbone Lever-Arm Effect Enhances Polymer Mechanochemistry. *Nat. Chem.* **2013**, *5*, 110-114.

(44) Kouznetsova, T. B.; Wang, J.; Craig, S. L. Combined Constant-Force and Constant-Velocity Single-Molecule Force Spectroscopy of the Conrotatory Ring Opening Reaction of Benzocyclobutene. *ChemPhysChem* **2017**, *18*, 1486-1489.

(45) Gossweiler, G. R.; Kouznetsova, T. B.; Craig, S. L. Force-Rate Characterization of Two Spiropyran-Based Molecular Force Probes. *J. Am. Chem. Soc.* **2015**, *137*, 6148-6151.

(46) Makarov, D. E. Perspective: Mechanochemistry of Biological and Synthetic Molecules. *J. Chem. Phys.* **2016**, *144*, 030901.

(47) Klein, I. M.; Husic, C. C.; Kovács, D. P.; Choquette, N. J.; Robb, M. J. Validation of the CoGEF Method as a Predictive Tool for Polymer Mechanochemistry. *J. Am. Chem. Soc.* **2020**, *142*, 16364-16381.

(48) Wohl, C. J.; Kuciauskas, D. Isomerization Dynamics of Photochromic Spiropyran Molecular Switches in Phospholipid Bilayers. *J. Phys. Chem. B* **2005**, *109*, 21893-21899.

(49) Caruso, M. M.; Davis, D. A.; Shen, Q.; Odom, S. A.; Sottos, N. R.; White, S. R.; Moore, J. S. Mechanically-Induced Chemical Changes in Polymeric Materials. *Chem. Rev.* **2009**, *109*, 5755-5798.

(50) Hinckley, D. A.; Seybold, P. G. A Spectroscopic/Thermodynamic Study of the Rhodamine B Lactone ⇌ Zwitterion Equilibrium. *Spectrochim. Acta A.* **1988**, *44*, 1053-1059.

(51) Traven, V. F.; Dolotov, S. M.; Ivanov, I. V. Activation of Fluorescence of Lactone Forms of Rhodamine Dyes by Photodehydrogenation of Aryl(hetaryl)pyrazolines. *Russ. Chem. Bull., Int. Ed.* **2016**, *65*, 735-740.

(52) Stauch, T.; Dreuw, A. Advances in Quantum Mechanochemistry: Electronic Structure Methods and Force Analysis. *Chem. Rev.* **2016**, *116*, 14137-14180.

Table of Contents

aromatic fusion of bis-mechanophore